ACS Macro Letters

Letter

pubs.acs.org/macroletters

Mechanical Activation of Mechanophore Enhanced by Strong Hydrogen Bonding Interactions

Yinjun Chen,† Huan Zhang,† Xiuli Fang, Yangju Lin, Yuanze Xu, and Wengui Weng*

Department of Chemistry, College of Chemistry and Engineering, Xiamen University, Xiamen 361005, People's Republic of China

Supporting Information

ABSTRACT: A mechanically active spiropyran (SP) mechanophore is incorporated into the backbone of prepolymer which is further end-capped with ureidopyrimidinone (UPy) or urethane. Strong mechanochromic reaction of SP arises in the bulk films of UPy containing materials whereas much weaker activation occurs in urethane containing counterparts, coincident with their stress−strain responses. The difference in the magnitudes of supramolecular interactions leads to different degrees of chain orientation and strain induced crystallization (SIC) in the bulk and consequently distinct capabilities to transfer the load to the mechanophores. This study may aid the design of novel mechanoresponsive materials whose mechanoresponsiveness can be tailored by tuning supramolecular interactions.

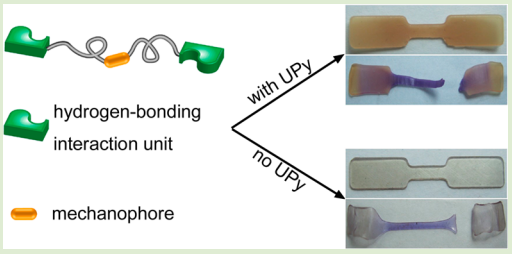

Mechanochemistry, the use of mechanical force instead of conventional stimuli (i.e., heat, light, and electricity) to activate chemical bonds, has attracted a great deal of interest in the past few years.[1−4] A considerable part of this field focuses on searching of mechanically functional molecules, that is, mechanophores. Mechanophores are often embedded into polymer chains which act like holders for macroscopic force. Rational design of the mechanophores and polymer architectures turns on a new route toward novel functions and products that are difficult to be accessed by other means.[1] In fact, a variety of novel functions have been successfully demonstrated by the mechanical activation of polymer-linked mechanophores, including biased reactivity,[5] force sensing,[6−11] reconfiguration of stereoisomers,[12] mechanical-triggered release of small molecules,[13−15] self-healing,[16−18] catalysis,[18−20] remodeling of polymers,[21,22] radical stabilization,[23] and chemiluminescence,[24] among others.[25−30] In spite of these fruitful developments, fewer efforts have been directed to understand the factors that influence the mechanical activation of polymer-linked mechanophores, especially in the bulk.

Pioneer works on polymer degradation and recent studies on mechanophore activation by sonication in dilute solution have demonstrated that the mechanical activation of chemical bonds is governed by single chain dynamics,[31−33] which depends on the rigidity of the backbone,[26] molecular weight and the quality of the solvent.[34] During sonication, high extensional rate is generated due to the collapse of cavitation bubbles.[35,36] When the extensional rate is faster than the relaxation speed of polymer chain, that is, the reciprocal of the longest relaxation time, the chain undergoes a coil-to-stretch transition that will elongate individual chemical bonds and activate the mechanophores.[34]

The mechanical activation of mechanophores in the bulk is less understood than that in solution owing to its complexities. Chain entanglements, phase separation, crystallization, intra- and interchain interactions, and so on, all can affect the effective load transfer to mechanophores. Moore and co-workers have covalently incorporated spiropyran (SP) into different polymer chains to create mechanoresponsive materials.[6−10] They further exploited the effects of linking site,[6,8] glass transition temperature,[7] locations in the blocks,[10] and strain rate[6,8,37] on the mechanical activation of SP. Our group recently designed a microphase separation mediated mechanical activation of SP in triblock copolymers.[38] We also incorporated both hydrogen bonding ureidopyrimidinone (UPy) and covalent mechanochromic SP into the polymer backbone to afford a novel polymeric material with superb mechanical performance and stress sensing functionality.[39] Herein, we demonstrate, for the first time, that the mechanical activation of mechanophores in the bulk can be enhanced by supramolecular interactions using strong UPy-based hydrogen bonding moieties attached to the polymer chain ends.

Our supramolecular design is based on macromers of SP containing prepolymers end-functionalized with UPy moieties that are decorated with two urea and one urethane motifs (Figure 1) primed for lateral hydrogen bonding.[40−42] Two different macromers were synthesized and denoted as **U10** and **U20** (Figures S6−S8) in which the numbers 10 and 20 are the approximate molecular weights of the prepolymers in kDa (Tables S1 and S2). Experimentally, the two hydroxyl groups of SP (Figures S1 and S2) were first completely reacted with a large excess of 1,6-hexyldiisocyanate (HDI). The mixture was then reacted with dihydroxyl poly(tetrahydrofuran) (PTHF, M_n = 2000 g mol^{-1}) to form isocyanate functionalized prepolymers. The prepolymers were then end-capped with UPy-1-(6-

Received: November 21, 2013
Accepted: January 10, 2014
Published: January 14, 2014

   dx.doi.org/10.1021/mz400600r | ACS Macro Lett. 2014, 3, 141−145

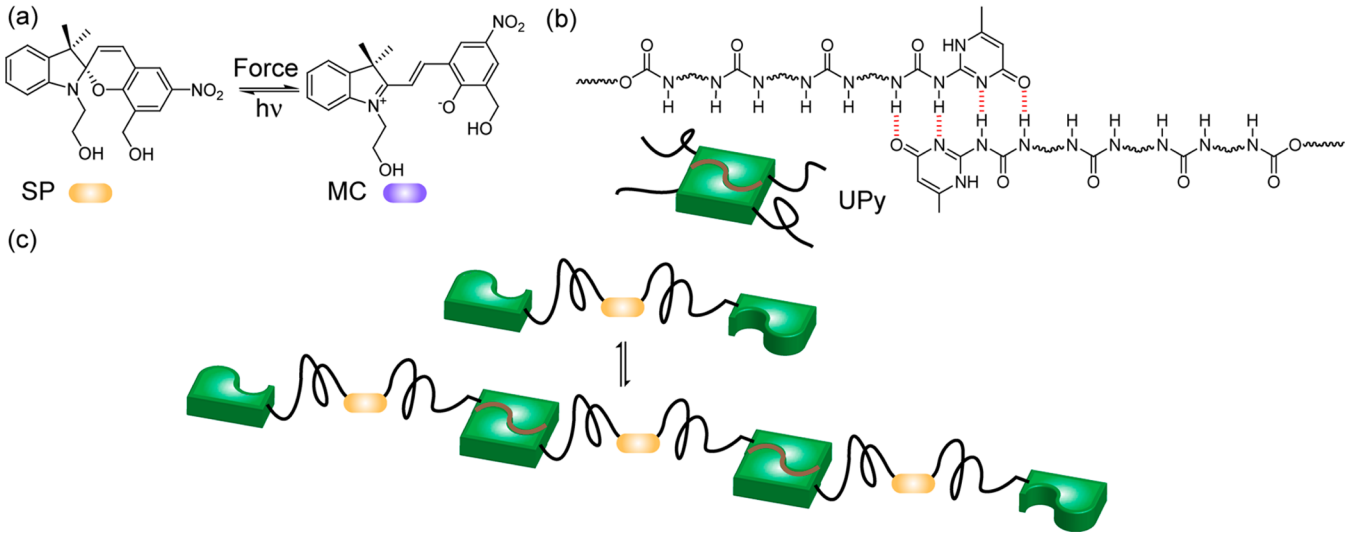

Figure 1. (a) Mechanochemical reaction from SP form to MC form activated by mechanical force. (b) Chemical structures of UPy containing macromer (only part of the chain was depicted for clarity). (c) Illustration of supramolecular polymerization of SP containing macromers.

aminohexyl)-3-pentylurea synthon (Figures S3–S5) to afford the target macromers. To emphasize the strength of the supramolecular interactions, the prepolymers were also reacted with ethanol instead of the UPy synthon, yielding two control polymers (**E10** and **E20**) end-functionalized with two urethane motifs (Figure S6). Films were then prepared via solution casting in Teflon casters and subsequent drying for 2 days in vacuo.

The morphology of solution-casted films of the supramolecular polymers and controls were first studied by small-angle X-ray scattering (SAXS). Shoulder peaks are present in **U10** and **U20** (Figure 2a). This is ascribed to the stacking of UPy dimers (Figure S11) and their phase separation from PTHF to form hard domains.[42] The precise peak positions q^* were evaluated from a Lorentz-corrected plot[43] (Figure S21) to be 0.47 and 0.49 nm^{-1} for **U10** and **U20**, respectively. The values of average interdomain distance d are 13.1 and 12.8 nm accordingly, close to literature reports.[42] These hard domains are randomly orientated, as evidenced by the isotropic 2D SAXS patterns (Figures 2a and S22). The soft/hard morphology were further found to be thermally labile (Figures S17–S19 and Figures S23–S26) due to the melting of lateral hydrogen bonds at high temperature.[42] Phase separation in **E10** and **E20** is not as significant as in **U10** and **U20** under the same conditions.

The effect of supramolecular polymerization as well as phase separation on the mechanical properties of the materials was then explored. The stress–strain responses of the four materials are shown in Figure 2b. The curves of **U10** and **U20** exhibit typical sigmoid shape for elastic polymers and take on significant strain-hardening behavior at large strain (arrows in Figure 2b), which is less obvious in **E10** and **E20**. **U10** and **U20** emerged superior mechanical performance in four parameters, that is, Young's modulus, ultimate strength, strain at break, and toughness, over **E10** and **E20** by virtue of the strong hydrogen bonding interactions (Table S3). For example, the toughness of **U20** (175 MPa) is 8 times that of **E20** (21.6 MPa).

We further turned to study the effect of strong supramolecular interactions on the mechanical activation of SP. No color varied when the engineering strain ε_{eng} was small. As ε_{eng} exceeded a critical strain value (denoted as ε_{onset}, Figures S12–

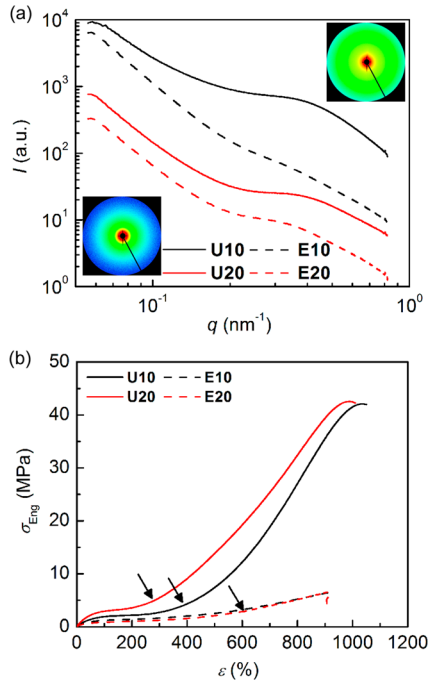

Figure 2. (a) SAXS results from the UPy containing materials (solid curves) and the controls samples (dashed lines). Curves are vertically shifted for clarity. Inlets are typical 2D scattering patterns of **U10** (up right) and **E10** (bottom left) in logarithmic scale. (b) The corresponding stress–strain responses. The arrows indicate the start of strain-hardening.

S15), pale blue developed from the middle of the sample, indicating the mechanochemical transduction from SP form to MC form. The extent of mechanical activation of the four materials after failure can be also judged from optical images shown in Figure 3a–d. Specimens from **U10** and **U20** displayed much more intense blue purple color in the gauge sections than **E10** and **E20**, implying a much higher degree of conversion from SP to MC in UPy containing materials than in the control materials. To further confirm the result, four materials were stretched under a much lower strain rate (0.0017

dx.doi.org/10.1021/mz400600r | ACS Macro Lett. 2014, 3, 141–145

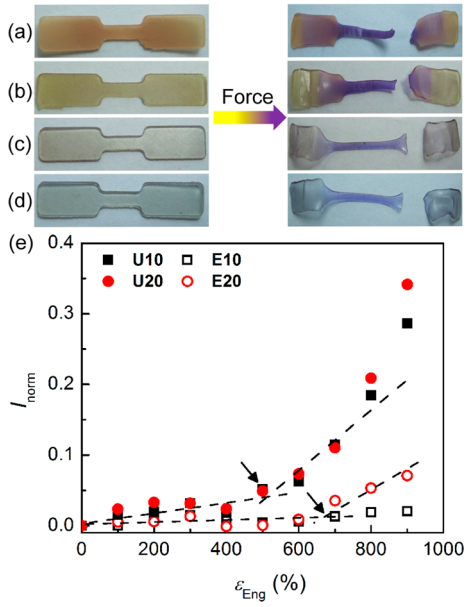

Figure 3. Mechanochromic response of the four materials (a) **U10**, (b) **U20**, (c) **E10**, and (d) **E20** after mechanical failure under a strain rate of 0.05 s^{-1}. (b) The normalized fluorescent intensity I_{norm} as a function of strain for **U10**, **U20**, **E10**, and **E20**. The black arrows indicate ε_{onset}.

s^{-1}, Figure S16) and **U10** and **U20** again showed superior mechanical activation over **E10** and **E20**.

According to literature,[44] the ring-opened MC form has two characteristic peaks at 578 and 620 nm in the emission spectrum. We then chose the peak intensity at 620 nm (denoted as I_{620}) to represent the amount of MC (Figures S30–S33) and monitored it as a function of ε_{eng}. We further transformed all SP units into MC form by UV light[9] and recorded the corresponding peak intensity as I_{620UV}. The normalized fluorescent intensity I_{norm} is expressed as $(I_{620}(\varepsilon_{eng}) - I_{620}(\varepsilon_{eng} = 0))/(I_{620UV} - I_{620}(\varepsilon_{eng} = 0)$; see Supporting Information), which gives the molar fraction of mechanically activated SP and is displayed in Figure 3e. The fractions of mechanically activated SP in **U10** and **U20** are 4–5× higher than those in **E10** and **E20** near fracture, respectively. For example, 34% SP is converted to MC for **U20** at ε_{eng} = 900%, whereas only 7% for **E20** at same strain. The values of ε_{onset} evaluated from the dashed extrapolation lines in Figure 3e are 500 and 670% for UPy containing materials and the controls, respectively. Interestingly, for all samples, ε_{onset} is well located inside the stress-hardening region (Figure 2b). Generally, strain-hardening is caused by highly oriented polymer chain[45] or by strain-induced crystallization (SIC). Therefore, our results suggest a strong interplay between the chain orientation or SIC and the mechanical activation of mechanophores.

Figure 4a shows the respective 2D SAXS patterns at selected strains for **U20**. Before deformation, the pattern is isotropic, indicating randomly oriented UPy stacks. With increasing strain, the UPy stacks rotate and fragment into smaller pieces by shear.[46] In the strain-hardening region, a bright streak appears along the equator direction (right angle to the tensile axis) as a result of reduced electron density contrast between the hard segments and the PTHF chains.[47] The SAXS pattern further revealed scattering lobes along the meridian direction (parallel to the stretching directions), showing the fragmented stacks were oriented perpendicular to the tensile axis with highly orientated soft segments lying parallel to the tensile axis (see Figures S27–S30 for more information).[46]

These highly oriented segments will further nucleate crystallization in the soft phases. Evidences of SIC of PTHF at high strain were found from differential scanning calorimetry (DSC) and wide-angle X-ray scattering (WAXS). Shown in Figure 4b,c are the DSC and WAXS of strained **U20** and **E20**. DSC revealed an additional melting endotherm peak around 45 °C for strained **U20** specimens. Meanwhile, the strained samples exhibited two sharp crystalline peaks at 2θ = 20 and 24° in WAXS pattern. Both DSC and WAXS results are consistent with literature reports on PTHF crystallization.[48,49] In contrast, **E20**, which is lacking strong supramolecular interactions, emerged no SIC even strained up to 700%.

Collectively, by introducing strong hydrogen bonding UPy to the chain ends, **U10** and **U20** exhibited mechanical and mechanochemical properties comparable to those of SP containing polyurethanes with covalent chain extenders.[10,39] Three main types of mechanically labile units are present in **U10** and **U20**: UPy stacks, UPy dimers, and SP. The UPy dimerization increases the "virtual" molecular weight of the supramolecular polymers **U10** and **U20**, while the stacking of UPy dimers leads to physical cross-linking. Both dimerization and stacking contribute to superior mechanical properties of **U10** and **U20**. The force required to break the UPy dimer is reported to be 100–200 pN,[50] which should be larger than that to break the UPy stacks (see Supporting Information) but is an order of magnitude lower than that to activate SP (2–3 nN[6]).

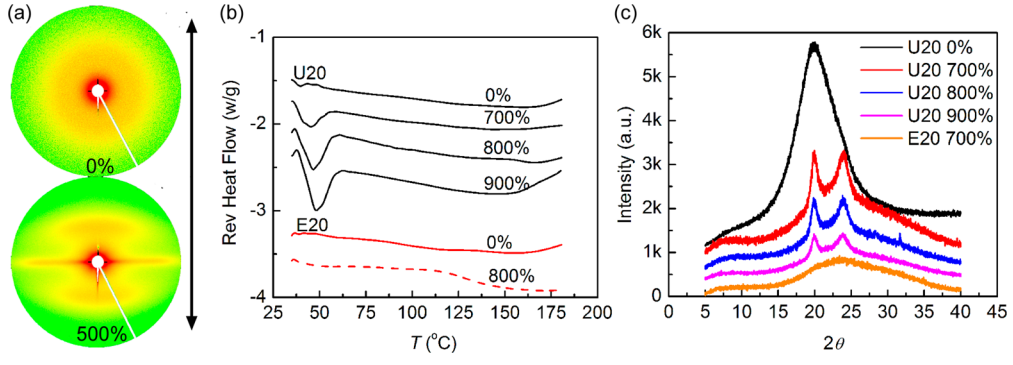

Figure 4. (a) 2D-SAXS patterns recorded from **U20** after straining to specified deformations indicated in the legend. The tensile (meridian) direction is vertical. (b) DSC measurement: reversible heat flow of **U20** and **E20** after different strains. (c) WAXS profiles of **U20** and **E20** at different strains.

dx.doi.org/10.1021/mz400600r | ACS Macro Lett. 2014, 3, 141–145

When **U10** and **U20** samples are subjected to tensile stretching, the randomly orientated stacks (Figure 5a) bear the load and

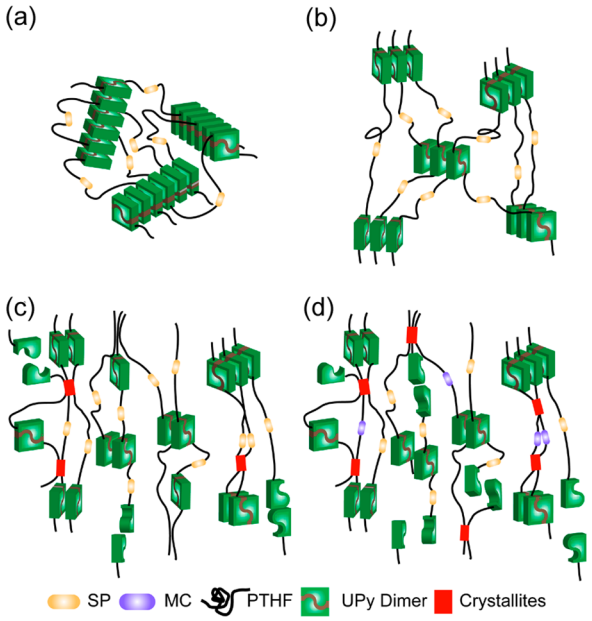

Figure 5. Proposed mechanism of mechanical activation in **U10** and **U20**; The stretching axis is vertical: (a) before stretching, (b) within strain-hardening region, (c) SIC of PTHF segments, and (d) mechanical activation of SP to MC.

are gradually shattered by shear stress.[46] As the strain steps into strain-hardening region, the fragments of the stacks are oriented perpendicular to the tensile direction, with soft segments lying parallel to the tensile axis (Figure 5b). The soft PTHF chains start to endure the load. Since the transient UPy dimer "chain extenders" are relatively strong and can slow the stress relaxation of the polymer chains, the orientation of the soft segments at large scale along the tensile direction is promoted. High degree segment orientation can initiate SIC. The resulting PTHF crystallites then act as additional cross-linkers to bear the majority of the load (Figure 5c). It is highly possible that only part of the UPy dimers is dissociated at this moment. Upon further stretching, the force is effectively transferred to SP, leading to mechanical activation and color change of the specimens (Figure 5d). Meanwhile, more and more dissociation of the UPy dimers occurs. On the other side, since there is no strong noncovalent association in **E10** and **E20**, stress relaxation of the short PU chains is much faster than that in **U10** and **U20**. Therefore, segment orientation is not significant and little or no SIC occurs in these controls during stretching (Figure 4b,c), leading to much less mechanical activation of SP.

In conclusion, mechanoresponsive SP have been incorporated into the backbone of prepolymer chains that were end-capped with UPy moieties. Significant SIC as well as mechanical activation of SP were observed in the bulk films of the UPy containing materials, whereas little or no SIC was found and weaker mechanical activation were observed in urethane motif end-capped control materials. This enhancement of mechanical activation of SP in UPy containing materials was ascribed to the strong supramolecular interactions promoted chain orientation and subsequent SIC. Our study may open a new way to create novel mechanoresponsive polymers whose mechanoresponsiveness can be controlled by tailoring the supramolecular interactions of the system.

■ ASSOCIATED CONTENT

Supporting Information

Synthetic details, NMR, DMA, SAXS, TGA, and additional information. This material is available free of charge via the Internet at http://pubs.acs.org.

■ AUTHOR INFORMATION

Corresponding Author

*E-mail: wgweng@xmu.edu.cn.

Author Contributions

†These authors contributed equally (Y.C. and H.Z.).

Notes

The authors declare no competing financial interest.

■ ACKNOWLEDGMENTS

This work was supported by National Natural Science Foundation of China (No. 21074103), the Fundamental Research Funds for the Central Universities (No. 2010121018), and Scientific Research Foundation for Returned Scholars. The authors greatly appreciate beamline BL16B1 (Shanghai Synchrotron Radiation Facility) for providing the beamtime and Dr. Feng Tian for the help of scattering experiment.

■ REFERENCES

(1) Black, A. L.; Lenhardt, J. M.; Craig, S. L. *J. Mater. Chem.* **2011**, *21*, 1655−1663.
(2) Caruso, M. M.; Davis, D. A.; Shen, Q.; Odom, S. A.; Sottos, N. R.; White, S. R.; Moore, J. S. *Chem. Rev.* **2009**, *109*, 5755−5798.
(3) Weder, C. *J. Mater. Chem.* **2011**, *21*, 8235−8236.
(4) Brantley, J. N.; Wiggins, K. M.; Bielawski, C. W. *Angew. Chem., Int. Ed.* **2013**, *52*, 3806−3808.
(5) Hickenboth, C. R.; Moore, J. S.; White, S. R.; Sottos, N. R.; Baudry, J.; Wilson, S. R. *Nature* **2007**, *446*, 423−427.
(6) Davis, D. A.; Hamilton, A.; Yang, J.; Cremar, L. D.; Gough, D. V.; Potisek, S. L.; Ong, M. T.; Braun, P. V.; Martínez, T. J.; White, S. R.; Moore, J. S.; Sottos, N. R. *Nature* **2009**, *459*, 68−72.
(7) Beiermann, B. A.; Davis, D. A.; Kramer, S. L. B.; Moore, J. S.; Sottos, N. R.; White, S. R. *J. Mater. Chem.* **2011**, *21*, 8443−8447.
(8) Kingsbury, C. M.; May, P. A.; Davis, D. A.; White, S. R.; Moore, J. S.; Sottos, N. R. *J. Mater. Chem.* **2011**, *21*, 8381−8388.
(9) Lee, C. K.; Davis, D. A.; White, S. R.; Moore, J. S.; Sottos, N. R.; Braun, P. V. *J. Am. Chem. Soc.* **2010**, *132*, 16107−16111.
(10) Lee, C. K.; Beiermann, B. A.; Silberstein, M. N.; Wang, J.; Moore, J. S.; Sottos, N. R.; Braun, P. V. *Macromolecules* **2013**, *46*, 3746−3752.
(11) O'Bryan, G.; Wong, B. M.; McElhanon, J. R. *ACS Appl. Mater. Interfaces* **2010**, *2*, 1594−1600.
(12) Wiggins, K. M.; Hudnall, T. W.; Shen, Q.; Kryger, M. J.; Moore, J. S.; Bielawski, C. W. *J. Am. Chem. Soc.* **2010**, *132*, 3256−3257.
(13) Baytekin, H. T.; Baytekin, B.; Grzybowski, B. A. *Angew. Chem., Int. Ed.* **2012**, *51*, 3596−3600.
(14) Diesendruck, C. E.; Steinberg, B. D.; Sugai, N.; Silberstein, M. N.; Sottos, N. R.; White, S. R.; Braun, P. V.; Moore, J. S. *J. Am. Chem. Soc.* **2012**, *134*, 12446−12449.
(15) Larsen, M. B.; Boydston, A. J. *J. Am. Chem. Soc.* **2013**, *135*, 8189−8192.
(16) Klukovich, H. M.; Kean, Z. S.; Iacono, S. T.; Craig, S. L. *J. Am. Chem. Soc.* **2011**, *133*, 17882−17888.
(17) Ramachandran, D.; Liu, F.; Urban, M. W. *RSC Adv.* **2012**, *2*, 135−143.

(18) Jakobs, R. T. M.; Ma, S.; Sijbesma, R. P. *ACS Macro Lett.* **2013**, *2*, 613−616.
(19) Piermattei, A.; Karthikeyan, S.; Sijbesma, R. P. *Nat. Chem.* **2009**, *1*, 133−137.
(20) Tennyson, A. G.; Wiggins, K. M.; Bielawski, C. W. *J. Am. Chem. Soc.* **2010**, *132*, 16631−16636.
(21) Lenhardt, J. M.; Black, A. L.; Craig, S. L. *J. Am. Chem. Soc.* **2009**, *131*, 10818−10819.
(22) Black Ramirez, A. L.; Ogle, J. W.; Schmitt, A. L.; Lenhardt, J. M.; Cashion, M. P.; Mahanthappa, M. K.; Craig, S. L. *ACS Macro Lett.* **2011**, *1*, 23−27.
(23) Lenhardt, J. M.; Ong, M. T.; Choe, R.; Evenhuis, C. R.; Martinez, T. J.; Craig, S. L. *Science* **2010**, *329*, 1057−1060.
(24) Chen, Y.; Spiering, A. J. H.; Karthikeyan, S.; Peters, G. W. M.; Meijer, E. W. *Nat. Chem.* **2012**, *4*, 559−562.
(25) Kryger, M. J.; Munaretto, A. M.; Moore, J. S. *J. Am. Chem. Soc.* **2011**, *133*, 18992−18998.
(26) Klukovich, H. M.; Kouznetsova, T. B.; Kean, Z. S.; Lenhardt, J. M.; Craig, S. L. *Nat. Chem.* **2013**, *5*, 110−114.
(27) Kean, Z. S.; Ramirez, A. L. B.; Yan, Y.; Craig, S. L. *J. Am. Chem. Soc.* **2012**, *134*, 12939−12942.
(28) Lenhardt, J. M.; Black, A. L.; Beiermann, B. A.; Steinberg, B. D.; Rahman, F.; Samborski, T.; Elsakr, J.; Moore, J. S.; Sottos, N. R.; Craig, S. L. *J. Mater. Chem.* **2011**, *21*, 8454−8459.
(29) Wiggins, K. M.; Syrett, J. A.; Haddleton, D. M.; Bielawski, C. W. *J. Am. Chem. Soc.* **2011**, *133*, 7180−7189.
(30) Brantley, J. N.; Wiggins, K. M.; Bielawski, C. W. *Science* **2011**, *333*, 1606−1609.
(31) Merrill, E. W.; Leopairat, P. *Polym. Eng. Sci.* **1980**, *20*, 505−511.
(32) Berkowski, K. L.; Potisek, S. L.; Hickenboth, C. R.; Moore, J. S. *Macromolecules* **2005**, *38*, 8975−8978.
(33) Potisek, S. L.; Davis, D. A.; Sottos, N. R.; White, S. R.; Moore, J. S. *J. Am. Chem. Soc.* **2007**, *129*, 13808−13809.
(34) Groote, R.; Szyja, B. M.; Pidko, E. A.; Hensen, E. J. M.; Sijbesma, R. P. *Macromolecules* **2011**, *44*, 9187−9195.
(35) Kuijpers, M. W. A.; Iedema, P. D.; Kemmere, M. F.; Keurentjes, J. T. F. *Polymer* **2004**, *45*, 6461−6467.
(36) Nguyen, T. Q.; Liang, O. Z.; Kausch, H. H. *Polymer* **1997**, *38*, 3783−3793.
(37) Beiermann, B. A.; Kramer, S. L. B.; May, P. A.; Moore, J. S.; White, S. R.; Sottos, N. R. *Adv. Funct. Mater.* **2013**, n/a−n/a.
(38) Jiang, S.; Zhang, L.; Xie, T.; Lin, Y.; Zhang, H.; Xu, Y.; Weng, W.; Dai, L. *ACS Macro Lett.* **2013**, 705−709.
(39) Fang, X.; Zhang, H.; Chen, Y.; Lin, Y.; Xu, Y.; Weng, W. *Macromolecules* **2013**, *46*, 6566−6574.
(40) Kautz, H.; Van Beek, D. J. M.; Sijbesma, R. P.; Meijer, E. W. *Macromolecules* **2006**, *39*, 4265−4267.
(41) Nieuwenhuizen, M. M. L.; de Greef, T. F. A.; van der Bruggen, R. L. J.; Paulusse, J. M. J.; Appel, W. P. J.; Smulders, M. M. J.; Sijbesma, R. P.; Meijer, E. W. *Chem.—Eur. J.* **2010**, *16*, 1601−1612.
(42) Appel, W. P. J.; Portale, G.; Wisse, E.; Dankers, P. Y. W.; Meijer, E. W. *Macromolecules* **2011**, *44*, 6776−6784.
(43) Stribeck, N. X-Ray Scattering of Soft Matter. In *X-Ray Scattering of Soft Matter*; Pasch, H., Ed.; Springer: New York, 2007; pp 117−118.
(44) Zhang, F.; Zou, X.; Feng, W.; Zhao, X.; Jing, X.; Sun, F.; Ren, H.; Zhu, G. *J. Mater. Chem.* **2012**, *22*, 25019−25026.
(45) Hoy, R. S.; Robbins, M. O. *J. Chem. Phys.* **2009**, *131*, 244901.
(46) Wisse, E.; Spiering, A. J. H.; Pfeifer, F.; Portale, G.; Siesler, H. W.; Meijer, E. W. *Macromolecules* **2009**, *42*, 524−530.
(47) Osman, A. F.; Edwards, G. A.; Schiller, T. L.; Andriani, Y.; Jack, K. S.; Morrow, I. C.; Halley, P. J.; Martin, D. J. *Macromolecules* **2012**, *45*, 198.
(48) Takahashi, H.; Shibayama, M.; Hashimoto, M.; Nomura, S. *Macromolecules* **1995**, *28*, 5547−5553.
(49) Rachmawati, R.; Woortman, A. J. J.; Loos, K. *Macromol. Biosci.* **2013**, *13*, 767−776.
(50) Guan, Z. B.; Roland, J. T.; Bai, J. Z.; Ma, S. X.; McIntire, T. M.; Nguyen, M. *J. Am. Chem. Soc.* **2004**, *126*, 2058−2065.